

Journal of Photonics for Energy

PhotonicsforEnergy.SPIEDigitalLibrary.org

Enhanced performance of dye-sensitized solar cells by omnidirectional antireflective coatings

Turkan Gamze Ulusoy
Bihter Daglar
Adem Yildirim
Amir Ghobadi
Mehmet Bayindir
Ali K. Okyay

SPIE.

Enhanced performance of dye-sensitized solar cells by omnidirectional antireflective coatings

Turkan Gamze Ulusoy,^{a,b} Bihter Daglar,^{a,b} Adem Yildirim,^{a,b}
Amir Ghobadi,^{a,c} Mehmet Bayindir,^{a,b,d} and Ali K. Okyay^{a,b,c,*}

^aBilkent University, UNAM–National Nanotechnology Research Center, Ankara 06800, Turkey

^bBilkent University, Institute of Materials Science and Nanotechnology, Ankara 06800, Turkey

^cBilkent University, Department of Electrical and Electronics Engineering,
Ankara 06800, Turkey

^dBilkent University, Department of Physics, Ankara 06800, Turkey

Abstract. Organically modified silica (ORMOSIL)-coated dye-sensitized solar cells (DSSCs) with improved energy conversion efficiency are demonstrated. ORMOSIL-coated DSSC surfaces exhibit omnidirectional low reflectivity over a broad range of wavelengths (400–800 nm). The short-circuit current density (J_{SC}) is enhanced up to 23% at normal incidence ($\theta = 0$ deg) as a result of ORMOSIL coating. In addition, J_{SC} enhancement is even higher at larger angles of incidence; 84% enhancement was observed at $\theta = 30$ deg. Moreover, ORMOSIL coating is superhydrophobic with a contact angle of 155 deg. © 2015 Society of Photo-Optical Instrumentation Engineers (SPIE) [DOI: [10.1117/1.JPE.5.053090](https://doi.org/10.1117/1.JPE.5.053090)]

Keywords: dye-sensitized solar cell; omnidirectional; antireflection coating; bioinspired nanostructures; photovoltaic technology.

Paper 15029 received Mar. 16, 2015; accepted for publication Jun. 1, 2015; published online Jun. 26, 2015.

1 Introduction

In the last decade, dye-sensitized solar cells (DSSCs) have undergone a renaissance as lightweight, low-cost, and relatively high efficiency photovoltaics (PV) due to extensive improvements in materials, device design and fabrication technologies.^{1,2} Intense research efforts mainly focused on synthesizing new organic dye molecules with higher absorptivity and materials as more efficient carrier transport layers.^{3–7} Single layer antireflection (SLAR) coating is a common approach to increase the light absorption in different types of solar cells.^{8–11} The use of silica micro/nanospheres,¹² bioinspired moth-eye shaped structures,¹³ and other designs are examples of these coatings.^{14,15} However, the SLAR coatings are optimized to decrease reflection losses in a relatively narrow spectral range and at incidence angles close to surface normal. On the other hand, solar radiation is inherently broadband and reaches the solar cell surface at a wide range of incidence angles. Therefore, broadband and omnidirectional AR coatings are required to provide significant enhancement in the device performance. Reflection from a surface can be significantly suppressed by gradually changing the refractive index between the two media.¹⁶ Although double layer,^{17,18} triple layer,¹⁹ multilayer coatings, and tapered structures²⁰ are proposed to achieve this gradual change, there are only limited reports^{8–11} that focus on the fabrication of graded index coatings on the surface of glass anode due to challenges such as high cost and suitability to large-area fabrication of such complex structures and their integration with DSSCs. The other challenge in preparing such multifunctional surfaces is to provide a trade-off between the high surface roughness requirement of superhydrophobic coatings and the low surface roughness requirement for antireflection capability.²¹ Therefore, to prepare antireflective and superhydrophobic surfaces, the roughness factor should be optimized; it must

*Address all correspondence to: Ali K. Okyay, E-mail: aokyay@ee.bilkent.edu.tr

be small enough to avoid diffuse reflection from the surface and high enough to provide superhydrophobicity.

Recently, we reported the facile fabrication of large-area organically modified silica (ORMOSIL) coatings with well-tuned porosity (therefore refractive index) and surface morphology.^{22,23} Due to their inherent porosity and hydrophobicity, these coatings demonstrate antireflective and/or superhydrophobic properties depending on their synthesis conditions. It is also possible to create multilayer ORMOSIL structures to realize omnidirectional and broadband AR coatings.²² In this letter, we demonstrate the integration of multilayer antireflective (MLAR) ORMOSIL coatings on the photoanode of a DSSC device. It is shown that MLAR ORMOSIL coatings can reduce light reflection losses in a broad range of wavelengths and angles of incidence that significantly improve the efficiency of DSSCs. For the proof-of-concept demonstration, we examine the applicability of this AR coating layer using commercial titania paste as photoanode. It should be noted that the substantial improvement in the cell efficiency can be attained through modification of each layer (such as using more absorptive dyes or highly collective photoanodes) or engineering of their interfaces to reduce carrier recombination, which is out of the scope of this paper. The results obtained here are of significant interest for commercialization issues, where self-cleaning and omnidirectionality of the layer guarantees the durability of the cell under harsh conditions and maximizes the solar exposure of the modules without using tilt and/or tracking systems.

2 Experimental Methods

Here, three-layer MLAR ORMOSIL coatings were chosen for their antireflective and self-cleaning properties. In brief, first and second layers present nanoporous structures (TM7.5 and TM60), while the third layer (at the bottom) presents a nonporous film (NPF). These layers were synthesized and coated according to our previous report.²²

2.1 Materials of Multilayer Antireflective Organically Modified Silica Coating

Tetraethyl orthosilicate (TEOS), tetramethyl orthosilicate (TMOS), methyltrimethoxysilane (MTMS), oxalic acid, and ammonium hydroxide (25%) were purchased from Merck (Germany), ethanol and hydrochloric acid (37%) (HCl) were purchased from Sigma-Aldrich (USA), and methanol was purchased from Carlo-Erba (Italy). All chemicals were used as received. Coatings were named indicating the TMOS volume fraction.

2.2 Preparation of Nanoporous Organically Modified Silica Coatings

To prepare ORMOSIL coatings, first ORMOSIL gels were synthesized.²³ ORMOSIL coatings were synthesized using MTMS and TMOS monomers with the complete hydrolysis and condensation, respectively. For first step, x mL (x is between 0.4 and 1) of MTMS and $1-x$ mL of TMOS are added to 9.74 mL of methanol. Afterward, 0.5 mL of 0.01 M aqueous oxalic acid solution is added up to the solution dropwise under gentle stirring. Furthermore, the mixture was stirred for 30 min and left for complete hydrolysis for 24 h at room conditions. Condensation was started by dropwise addition of 0.42 mL of ammonium hydroxide (25%) and 0.19 mL of water mixture under gentle stirring; it was stirred for 15 min. Finally, the solution was poured into a polystyrene vial and left for gelation process at room temperature. Gels were typically formed within 1 day, then to strengthen the porous structure, they were aged for 2 days. Afterward, 12 mL of methanol was added to the gel, and the resulting mixture was sonicated for 45 s at 20 W using an ultrasonic liquid homogenizer in order to obtain ORMOSIL colloids. The colloids were spin coated on clean glass surfaces at 2000 rpm and dried at room temperature overnight. To increase the hydrophobicity and integrity of the coatings, they were annealed to 450°C for 1 h. The colloids and corresponding coatings are named with the number in the abbreviation indicating the TMOS volume fraction in the corresponding colloid, such that TM 7.5 indicates the coating produced using the colloid containing 7.5% TMOS and 92.5% MTMS.

2.3 Preparation of Nonporous Organically Modified Silica Coatings

The third and last member of MLAR is NPF, which was prepared by TEOS and MTMS monomers according to standard procedure,²³ where 4.5 mL of MTMS (for NPF 1) or 3 mL of MTMS and 1.5 mL of TEOS (for NPF 2) were dissolved in 4.5 mL of ethanol and 0.4 mL of water, and 10 μL of 0.1 M HCl were added. The mixture was stirred (at 250 rpm) at 60°C for 90 min. Then 0.8 mL of 0.1 M HCl and 0.7 mL of water were added and further stirred for 15 min at room temperature. Then the solution remained at 50°C for 15 min and was diluted with an appropriate amount of ethanol. For example, to prepare 80-nm thick films, we added 14 mL of ethanol to the 2 mL of aged solution. Finally, 200 μL portions of diluted solution were coated on clean glass surfaces with spin coating at 2000 rpm.

2.4 Preparation of Three-Layer Coating

We prepared this three-layer AR coating by successive spin coating of ORMOSIL solutions at 2000 rpm. First, the nonporous ORMOSIL layer (NPF 2) was spin coated as described above and dried at room temperature overnight. After that, on top of this coating, 140-nm thick TM60 was coated. To obtain the desired thickness, 4 mL of TM 60 colloid was diluted using 3 mL of methanol. This layer was dried at 225°C for 1 h. Then \sim 240 nm TM 7.5 layer was coated on the top of the TM 60 layer. To give the desired thickness, 2 mL of TM 7.5 colloid was diluted using 1 mL of methanol. Finally, coating was cured at 450°C for 1 h to guarantee strong adhesion between the layer and glass substrate. Also, it should be noted that spin coating of the AR solution was carried out using a low-profile chuck with a fragment adapter (laurell 5–25 mm Adapter P/N 1002 0748 in NPP) and this mm-scale vacuum hole is adjusted to a place far from the TiO₂ paste. Hence, no damage was observed at the TiO₂ paste during the spin coating.

2.5 Dye-Sensitized Solar Cell Assembling

Nanoporous TiO₂ coated fluorine doped tin oxide (FTO) glass was purchased from Solaronix (\sim 8–10 μm , opaque) as a working electrode. Three-layer ORMOSIL colloids were then coated one by one on glass surfaces using a spin coating method and the photoanode was annealed at 450°C for 1 h to get titania anatase crystalline structure. After isolation of the ORMOSIL coated side, TiO₂ photoanodes were soaked in 0.5-mmol ruthenium sensitizer [cis-di(thiocyanato)-N-N'-bis(2,2'-bipyridyl)-4-carboxylic acid-4'-tetrabutylammonium carboxylate) ruthenium (II)] dye (known as N719, Solaronix) in a t-butanol/acetonitrile (1:1, in volume ratio) solution, for 24 h at room temperature. The samples were rinsed with acetonitrile to remove nonchemisorbed dye molecules. The drilled platinum-coated conducting glass was used as counter electrodes bonded to photoanode by 25- μm -thick thermal sealant (Dupont). The active area of each cell was filled with \sim 10 μL electrolyte (Iodalyte HI, Solaronix) driven by capillary force through the hole. The area of the electrode was controlled using a mask of 0.36 cm² area on the hot-melt sealed film. The projected area for the tilted angles is also taken to be 0.347 cm² and 0.312 cm² for 15 deg and 30 deg incidence angles, respectively.

3 Characterization

The complete PV devices have been characterized with current-voltage (I-V) measurement and incident photon-to-current conversion efficiency (IPCE). The I-V characteristics of the devices were measured using a Keithley 2400 source meter equipped with a solar simulator (Newport, model 67005) and air mass filter (AM 1.5 G) under a simulated solar light irradiation with an intensity of 100 mW/cm². For IPCE measurement, a 150 W Xenon lamp was used as a wideband illuminating source. Monochromatic light (Oriel 1/8 m cornerstone monochromator, 1200 lines/mm grating) was obtained and mechanically chopped at 5 Hz. The light was focused on the fabricated device and the solar cell had been biased with a Keithley 2400 source meter. The gate terminal voltage bias was independently controlled with a separate voltage supply (Keithley 2400). A lock-in amplifier (Stanford Research Systems 830) was used to measure the photogenerated current flowing between the anode and cathode terminals. Ideally,

connecting a lock-in amplifier in series and measuring the photocurrent was preferred. The incident optical beam spot (on the surface of the sample) was 400 μm wide and 1200 μm long.

In addition to this, a contact angle meter (OCA 30, data physics) was used to obtain static contact angles of coated samples and scanning electron microscope (SEM, FEI – Quanta 200 FEG, operated at 10 kV) had been employed to characterize the morphology and dimensions of the structure.

4 Results and Discussions

Superhydrophobic ORMOSIL aerogel thin films are reported as an effective route for large-area superhydrophobic AR layers. To the best of our knowledge, no integration of these coatings with a solar cell structure has been studied before. In this report, photoanode is functionalized with a three-layer AR coating and the effect of this coating on PV performance has been investigated. It is shown that this layer can significantly reduce the light loss, hence it enhances the efficiency of the solar cell.

Figure 1(a) illustrates a three-dimensional schematic of the fabricated photoanodes of dye sensitized solar cell that is functionalized by MLAR ORMOSIL coating. The proposed device consists of five main parts: (1) broadband and omnidirectional MLAR ORMOSIL coating for matching the refractive indices of air ($n = 1$) and glass ($n = 1.5$), (2) nanoporous titania paste on transparent conducting oxide (TCO) as photoanode, (3) cis-bis (isothiocyanato) bis

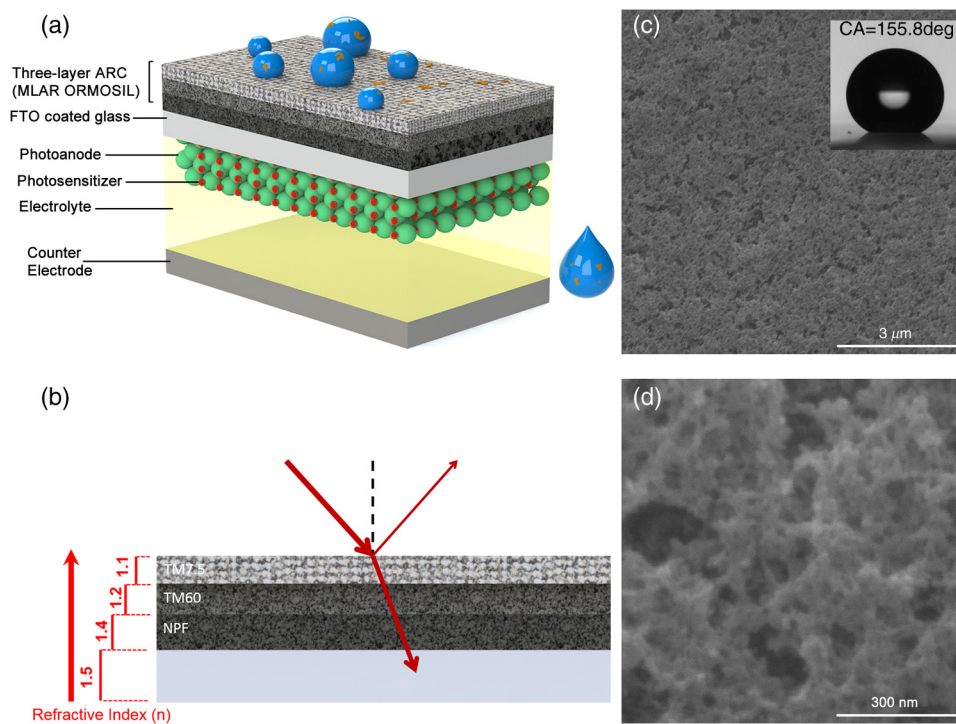


Fig. 1 (a) Schematic of the dye sensitized solar cell (DSSC) design consists of multilayer AR (MLAR) organically modified silica (ORMOSIL) coating (three-layer antireflective (AR) coating) single side coated transparent conducting oxide (TCO) glass substrate, titania paste as photoanode, dye as photosensitizer, electrolyte as electron transfer mediator, and Pt-coated conducting glass as counter electrode. This AR coating which is a superhydrophobic porous film can provide self-cleaning property of the cell, blue spheres and brown particles on the surface represent the water droplets and dirt molecules, respectively. (b) The schematic illustration of AR coating with three layers and its effect on light reflection reduction through gradual increasing of the refractive indices as 1.1, 1.2, 1.4, respectively, to match it to the bare glass refractive index (1.5). (c) Top view scanning electron microscope (SEM) images of three-layer porous thin film. The inset shows the water contact angle of the surface, which is 156 deg, indicating superhydrophobic property of the porous film. (d) Higher magnification SEM image of the surface.

(2,2'-bipyridyl-4,4'-dicarboxylato) ruthenium (II) (N719) as photosensitizer, (4) the iodide/tri-iodide (I^-/I_3^-) shuttle as electron transfer mediator, and finally (5) Pt-coated conducting glass as counter electrode.

Figure 1(b) shows the working principle of AR coated photoanode. Previously, we determined that the optimum refractive indices of the bottom layer (NPF), middle layer (TM60), and top layer (TM7.5) were ~ 1.4 , ~ 1.2 , and ~ 1.1 , respectively, and corresponding thicknesses were determined to be 80, 140, and 240 nm, respectively.²² The gradual matching of the refractive index of air ($n = 1$) to the glass minimizes the reflection of the light from the surfaces and accordingly increases the light absorption of the cell. Scanning electron microscope (SEM) images of the three-layer ORMOSIL coating on a TCO substrate are shown in Figs. 1(c) and 1(d). The nanoporous structure of the MLAR also utilizes a self-cleaning property with a contact angle of ~ 156 deg [Fig. 1(c) inset] owing to its superhydrophobicity. This finding is promising for the outdoor application of such DSSCs to prevent dirt accumulation on the devices.

In order to investigate the impact of multifunctional ORMOSIL coating and its omnidirectional property on the PV performance of the DSSCs, current-voltage curves were collected at different angles of light incidence (0 deg, 15 deg, 30 deg). The DSSC without AR coating was prepared by removing the coating to use identical solar cells as its own reference cell in both measurements. Due to its hybrid nature, this ORMOSIL coating is deformable, mechanically and thermally stable and makes strong adhesion to the plastic and glass substrates.^{23,24} A further improvement in the adhesion between glass and the coating was also attained through annealing at 450°C for 1 h. Therefore, to remove this coating from the surface, first, we gently scrapped it off using razor blade for a couple of times. After partial removal of the coating, the residues were taken away from the surface using acetone and cleanroom swabs. Also, the quality of the surface was compared with a bare glass, using UV-V is spectroscopy, demonstrating almost the same transmittance for both samples (not given here). Figures 2(b)–2(d) compare the solar cell current density-voltage ($J_{SC} - V$) characteristics in the absence and presence of AR coating. All related parameters including the short-circuit current density (J_{SC}), fill factor (FF), and overall conversion efficiency (η) were summarized in Table 1. These results prove that by applying this multifunctional coating on DSSCs, obvious increments in short-circuit current density (J_{SC}) and efficiency (η) were attained for all different angles of incidence.

For normally incident incoming light ($\theta = 0$ deg), the device achieves a J_{SC} improvement of $\sim 23\%$ which results in an efficiency rise of $\sim 25.9\%$. This ratio shows an upward trend and is more salient for larger angles of incidence which is triggered by the absorption of more photons due to lower surface reflection and reaches 32.1% ($\Delta\eta = 31.1\%$) and 84.6% ($\Delta\eta = 94\%$) for 15 deg and 30 deg, respectively.

Enhanced J_{SC} values as well as IPCE efficiency of the MLAR ORMOSIL coated DSSCs are closely related to the improvement of their transmittance and light absorption characteristics of the photoanodes with MLAR ORMOSIL coatings. Improvement in J_{SC} can be explained using

Table 1 Photovoltaic (PV) parameters for the organically modified silica (ORMOSIL) coated photoanode in dye sensitized solar cell (DSSC) at different angles of incidence under AM 1.5 G filtered spectral illumination at incident intensity of 100 mW/cm².

Device	Angle θ	V_{OC} (V)	J_{SC} (mA/cm ²)	FF	η (%)
ORMOSIL coated	0	0.59	4.66	0.67	1.85
uncoated	0	0.59	3.79	0.66	1.47
ORMOSIL coated	15	0.59	4.13	0.67	1.62
uncoated	15	0.59	3.16	0.66	1.23
ORMOSIL coated	30	0.57	2.77	0.70	1.12
uncoated	30	0.57	1.50	0.67	0.57

Note: Reference cell (uncoated cell) = DSSC removed the coating using a razor blade for each cell. Values given are mean values of three cells prepared in a similar way. Experimental errors of the mean values are within ± 2 mV for V_{OC} , ± 0.20 mA/cm² for J_{SC} , and $\pm 0.5\%$ for FF.

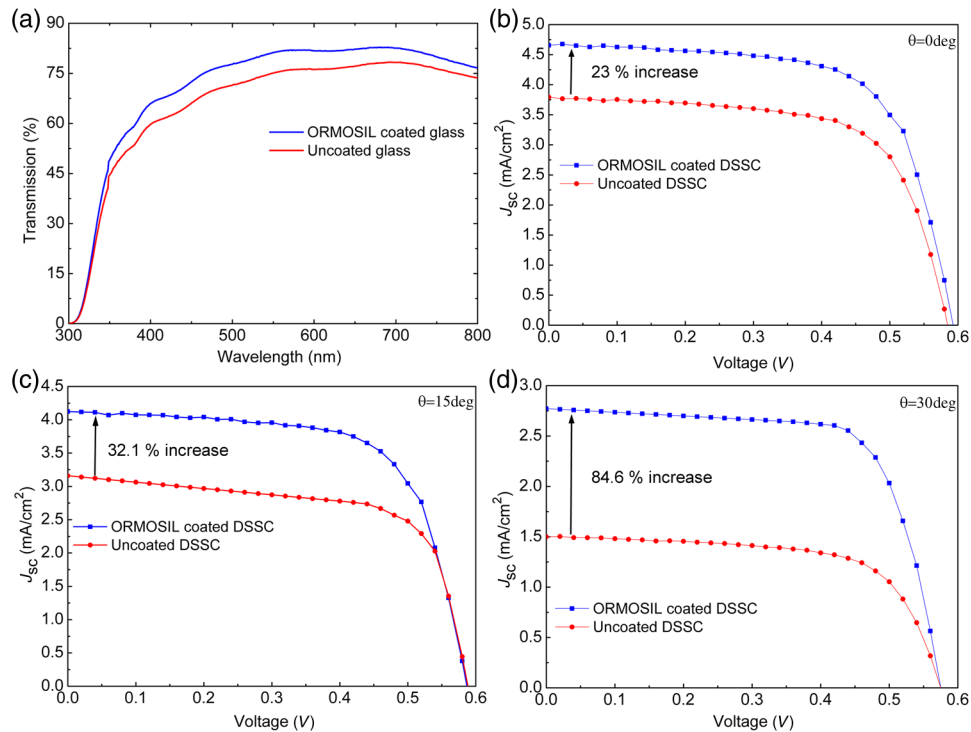


Fig. 2 (a) Variations of UV-Vis optical transmittance spectra for the ORMOSIL coated (blue) and uncoated (red) samples. For the whole range, 300–800 nm, the amount of transmittance has increased and an average increase of 6.5% is recorded for visible spectrum. (b-d) One-to-one comparison of current-voltage ($J_{SC} - V$) characteristics of the ORMOSIL coated cells under different incident angles of incoming wave (0 deg, 15 deg, 30 deg) at 100 mW/cm². The ORMOSIL coating has been removed by razor blade and acetone and used as the uncoated sample. It is shown that the amount of J_{SC} has increased by 23%, 32.1%, and 84.6% for different incident angles of 0 deg, 15 deg, and 30 deg, respectively.

the nonlinear relation between the number of generated carriers due to the photon absorption and J_{SC} in DSSCs.²⁵ The transmission spectra of both ARC coated and uncoated FTO coated glass samples have been illustrated in Fig. 2(a). As can be seen, ORMOSIL film has increased the amount of transmitted light from air to glass interface. When this coating is applied to our device, an average increase of 6.5% in generated electrons made an enhancement in J_{SC} as much as 23%. In previous reports,²⁵ it was shown that the relation between number of generated carriers (Q) and J_{SC} can have a nonlinear form, in which J_{SC} is proportional to Q^α , where $\alpha (> 1)$ is a coefficient that depends on the material and device properties of the DSSC. Therefore, the slight increase in the amount of transmittance could lead to a considerable change in the J_{SC} .

Moreover, in our previous study, it has been shown that the AR layer reduces the light reflected off the surface, which is lower than 2% on average (in the desired frequency ranging from 400 to 700 nm) over all incoming incident angles. Reflection loss increases considerably when moving to more oblique angles, which means that the suppression of light reflection is more dominant for higher angles of incidence. Keeping this in mind, it is expected that the J_{SC} enhancement of the DSSC is more significant for oblique angles, while open-circuit voltage, V_{OC} , does not change with the use of the three-layer coating. Considering the fact that V_{OC} is mainly related to the retardation of the electron's back reaction at the semiconductor/electrolyte interface and our modification is not related to this interface, it is expected that V_{OC} is almost constant (between 0.57 and 0.59) for all measurements.

In addition to earlier explanations, the substantial increase in J_{SC} can be understood by the spectral IPCE measurement shown in Fig. 3. As expected, the ORMOSIL functionalized DSSC has sufficiently higher IPCE values compared to the reference device which is in accordance with our earlier results.

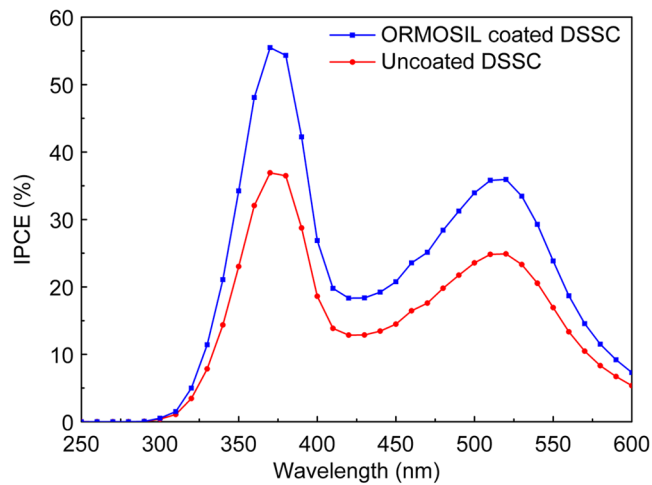


Fig. 3 Incident photon-to-current conversion efficiency (IPCE) curves are collected in a wavelength ranging from 250 to 600 nm for the both ORMOSIL coated and uncoated cells. The amplitude of maximums located at 370 and 520 nm are improved by about 19% and 11%, respectively. The three-layer coating significantly improves IPCE efficiency for the solar cell.

5 Conclusions

In summary, we demonstrate the fabrication of large-area multilayer ORMOSIL coated DSSCs with omnidirectional, broadband antireflection, and self-cleaning properties. We showed that the measured improvements in J_{SC} as a function of incident light angle (0 deg, 15 deg, and 30 deg) and achieving an averaged J_{SC} improvement of 84.6% for a high oblique angle as much as 30 deg, stemming from enhanced transmittance and higher light absorption of the photoanode. The presented results affirm that such a nanostructured coating can be a promising idea for future performance-enhanced solar cells not only due to improving the PV performance of the cell but also for its self-cleaning property, which renders it an excellent option for outdoor applications.

Acknowledgments

This work was supported by the Scientific and Technological Research Council of Turkey (TUBITAK) under Grant Nos. 109E044, 111T696, 112M004, 112E052, and 113M815. A.K.O. acknowledges support from the Turkish Academy of Sciences Distinguished Young Scientist Award (TUBA GEBIP). T.G.U. thanks TUBITAK-BIDEB 2210-C for MS scholarship.

References

1. S. Zhang et al., "Highly efficient dye-sensitized solar cells: progress and future challenges," *Energy Environ. Sci.* **6**, 1443–1464 (2013).
2. B. E. Hardin, H. J. Snaith, and M. D. McGehee, "The renaissance of dye-sensitized solar cells," *Nat. Photonics* **6**, 162–169 (2012).
3. N. Robertson, "Optimizing dyes for dye-sensitized solar cells," *Angew. Chem. Int. Ed. Engl.* **45**, 2338–2345 (2006).
4. D. Kuang et al., "High molar extinction coefficient heteroleptic ruthenium complexes for thin film dye-sensitized solar cells," *J. Am. Chem. Soc.* **128**, 4146–4154 (2006).
5. U. Bach et al., "Solid-state dye-sensitized mesoporous TiO₂ solar cells with high photon-to-electron conversion efficiencies," *Nature* **395**, 583–585 (1998).
6. Q. Zhang and G. Cao, "Nanostructured photoelectrodes for dye-sensitized solar cells," *Nano Today* **6**, 91–109 (2011).
7. R. Y. Ogura et al., "High-performance dye-sensitized solar cell with a multiple dye system," *Appl. Phys. Lett.* **94**, 073308 (2009).

8. X. Yan et al., "Enhanced omnidirectional photovoltaic performance of solar cells using multiple-discrete-layer tailored- and low-refractive index anti-reflection coatings," *Adv. Funct. Mater.* **23**, 583–590 (2013).
9. J. Y. Lee et al., "Simple approach for enhancement of light harvesting efficiency of dye-sensitized solar cells by polymeric mirror," *Opt. Express* **18**, 510 (2010).
10. H. Li et al., "Antireflective photoanode made of TiO₂ nanobelts and a ZnO nanowire array," *J. Phys. Chem. C* **114**, 11375–11380 (2010).
11. U. Gangopadhyay et al., "Antireflective nanocomposite based coating on crystalline silicon solar cells for building-integrated photovoltaic systems," *Hindawi Conf. Pap. Energy*, 1–6 (2013).
12. M. Tao et al., "Surface texturing by solution deposition for omnidirectional antireflection," *Appl. Phys. Lett.* **91**, 081118 (2007).
13. K. M. Yeung et al., "2-step self-assembly method to fabricate broadband omnidirectional antireflection coating in large scale," *Sol. Energy Mater. Sol. Cells* **95**, 699–703 (2011).
14. M. Chigane, Y. Hatanaka, and T. Shinagawa, "Enhanced antireflection properties of silica thin films via redox deposition and hot-water treatment," *Sol. Energy Mater. Sol. Cells* **94**, 1055–1058 (2010).
15. C. Ballif et al., "Solar glass with industrial porous SiO₂ antireflection coating: measurements of photovoltaic module properties improvement and modelling of yearly energy yield gain," *Sol. Energy Mater. Sol. Cells* **82**, 331–344 (2004).
16. B. Daglar et al., "Soft biomimetic tapered nanostructures for large-area antireflective surfaces and SERS sensing," *J. Mater. Chem. C* **1**, 7842–7848 (2013).
17. Z. Liu et al., "Sol-gel SiO₂/TiO₂ bilayer films with self-cleaning and antireflection properties," *Sol. Energy Mater. Sol. Cells* **92**, 1434–1438 (2008).
18. N. F. Wang et al., "Porous SiO₂/MgF₂ broadband antireflection coatings for superstrate-type silicon-based tandem cells," *Opt. Express* **20**, 7446 (2012).
19. M. H. Asghar et al., "Design and preparation of antireflection films on glass substrate," *Turk. J. Phys.* **29**, 43–53 (2005).
20. Y. Ohtera, D. Kurniatan, and H. Yamada, "Antireflection coatings for multilayer-type photonic crystals," *Opt. Express* **18**, 12249–12261 (2010).
21. K. L. Cho et al., "Influence of roughness on a transparent superhydrophobic coating," *J. Phys. Chem. C* **114**, 11228–11233 (2010).
22. A. Yildirim et al., "Superhydrophobic and omnidirectional antireflective surfaces from nanostructured ORMOSIL colloids," *ACS Appl. Mater. Interfaces* **5**, 853–860 (2013).
23. H. Budunoglu et al., "Highly transparent, flexible, and thermally stable superhydrophobic ORMOSIL aerogel thin films," *ACS Appl. Mater. Interfaces* **3**, 539–545 (2011).
24. H. S. Lim et al., "Multifunctional hybrid fabrics with thermally stable superhydrophobicity," *Adv. Mater.* **22**, 2138–2141 (2010).
25. G. Schlichthorl, N. G. Park, and A. J. Frank, "Evaluation of the charge-collection efficiency of dye-sensitized nanocrystalline TiO₂ solar cells," *J. Phys. Chem. B* **103**, 782–791 (1999).

Turkan Gamze Ulusoy received her BS degree in chemical engineering from Ankara University, Ankara, Turkey, in 2012. She is pursuing her master's degree under the guidance of professor Ali K. Okyay in UNAM, National Nanotechnology Research Center, Institute of Materials Science and Nanotechnology at Bilkent University. Her current research interests include design, fabrication, and characterization of solar-light driven clean energy materials for photocatalysis and solar cells.

Bihter Daglar received her BS degree in chemical engineering from Hacettepe University in 2007, and her MS degree in chemical engineering from Hacettepe University in 2010. Since 2010, she has been a PhD student in Bilkent University Institute of Materials Science and Nanotechnology, under the supervision of Dr. Mehmet Bayindir. Her research interests include fabrication of nanostructured and functional surfaces, synthesis of nanoparticles, and chemical sensors.

Adem Yildirim received his BS degree in chemical engineering from Hacettepe University in 2007 and his MS and PhD degrees in materials science and nanotechnology from Bilkent

University in 2009 and 2014, respectively. Since January 2015, he has been working as a post-doctoral researcher in the Chemical and Biological Engineering Department at the University of Colorado, Boulder. His research interests include synthesis of nanostructured silica materials, interactions between nanomaterials and biological systems, and ultrasound imaging.

Amir Ghobadi received his BS degree in electrical engineering from the University of Tehran, Iran, in 2012. He received his MS degree in electrical engineering from Bilkent University. Currently, he is working toward his PhD in the Department of Electrical and Electronics Engineering at Bilkent University, Turkey. His research involves the design, synthesis, and characterization of novel semiconductor-based photovoltaic devices.

Mehmet Bayindir received his PhD degree in physics from Bilkent University, Ankara, Turkey, in 2002. As a postdoctoral researcher and later research scientist at the Research Laboratory for Electronics/Massachusetts Institute of Technology (USA), Bayindir developed a new fabrication technique for making multimaterial, active in-fiber devices from metal, insulator, and semiconducting parts for the first time. After returning to his home country, he undertook the building of UNAM-National Nanotechnology Research Center and now serves as director of the center.

Ali K. Okyay received his BS degree from Middle East Technical University in 2001 and his MS and PhD degrees from Stanford University in 2003 and 2007, respectively, all in electrical engineering. He has been a faculty member at Bilkent University since 2008, holding joint appointment in electrical engineering at the UNAM-National Nanotechnology Research Center and the Institute of Materials Science and Nanotechnology. His research focuses on integrated devices and sensors. He has authored over 200 scientific journal and conference publications.